High-Performance Half-Heusler Thermoelectric Devices Through Direct Bonding Technique

Amin Nozariasbmarz, ** Udara Saparamadu, ** Wenjie Li, Han Byul Kang, Carter Dettor, Hangtian Zhu, Bed Poudel, ** Shashank Priya**

Department of Materials Science and Engineering, Pennsylvania State University, University Park, PA 16802, USA

These authors contributed equally to this work

* Corresponding Authors: Amin Nozariasbmarz (aln192@psu.edu), Bed Poudel (bup346@psu.edu) and Shashank Priya (sup103@psu.edu)

Abstract

Solid-state thermoelectric generators (TEGs) are promising solution for waste heat recovery. However, they typically suffer from lower conversion efficiency, lack of reliable high temperature device fabrication process and long-term stability. In order to realize high electrical conversion efficiency (ECE) in TEGs, it is critical that in conjunction with high TE materials figure of merit, zT, there is also a reliable TE module fabrication process. This study demonstrates the TEG fabrication process that results in reduced thermal and electrical contact resistances between metal electrodes and TE legs, even at high temperatures (>600°C). The fabrication approach is demonstrated using p-type ZrCoSb-based and n-type ZrNiSn-based half-Heusler TE materials. High temperature brazing material is used as a filler that enables direct bonding of TE legs to the copper electrode without metalizing legs. This technique improves the TEG performance and stability at high temperatures by minimizing the contact resistance and diffusion at TE leg/electrode interface. The fabricated modules exhibit a high power density of ~11.5 Wcm⁻² and an ECE of 9.5% at 670°C temperature gradient. The module was exposed to longtime soaking at

550°C in air and was found to exhibit negligible deterioration. These results are highly promising for advancing the TE modules in waste heat recovery applications.

Keywords: Waste heat recovery, Thermoelectric, half-Heusler, Contact resistance, Efficiency, Air stability, Direct bonding, Metallization

1. Introduction

Novel renewable and sustainable alternative energy resources are being developed by harvesting wasted energy [1,2,3]. Thermoelectric generators (TEGs) are promising for directly converting waste heat into electricity and are positioned to play a major role in providing energy harvesting solutions [2,4,5]. In past few decades, both theoretical and experimental research has been conducted on the development of thermoelectric (TE) materials [6,7,8]. TE material performance is evaluated by a dimensionless figure of merit, zT. High zT (≥ 1) has been a benchmark for high-performance TE materials. The maximum conversion efficiency (η) of a TE material is expressed by Equation (1) [9]

$$\eta = \left(\frac{T_H - T_C}{T_H}\right) \frac{\sqrt{1 + (zT)_{avg}} - 1}{\sqrt{1 + (zT)_{avg}} + \left(\frac{T_C}{T_H}\right)} \tag{1}$$

where T_C and T_H are cold- and hot-side temperatures, respectively, and $(zT)_{avg}$ is the average material figure of merit. The first term in parenthesis is the theoretical maximum efficiency, known as Carnot efficiency. Higher $(zT)_{avg}$ and ΔT (= T_H - T_C) leads to higher η in a desired temperature range.

Prior investigations have led to fundamental understanding of design principles, identification of promising material systems, and development of suitable synthesis techniques. This has led to demonstration of excellent material performances. For example – peak zT of 2.6 and 2.5 at 650°C has been reported in SnSe single crystal [10] and polycrystalline Na-doped PbTe-

SrTe alloys [11], respectively. (Bi,Sb)Te₃ [12,13,14,15] and Mg₃(Bi,Sb) [16,17,18] systems have been found to be excellent TE materials at low temperatures (-50 to 250°C). In medium temperature range (250 to 550°C), there are multiple options such as Ba₈Ga₁₆Ge₃₀ [19], Mg₂(Sn,Si,Ge) [3,20,21,22], BiCuSeO [23,24], Zn₄Sb₃ [25,26], Cu₂(S,Se,Te) [27,28], GeTe [29,30] and skutterudites [31,32,33,34,35]. In high temperature range (550 to 1000°C), SiGe [36,37,38,39], Yb₁₄MnSb₁₁ [40], and half-Heuslers [7,41,42,43,44,45] are suitable candidates. These material advancements have strengthened the opportunity for design and development of TE devices. However comparatively, the progress in fabricating high temperature TE devices has been limited and there is considerable gap between the reported zT values and device performance. A TE device comprises of several materials in addition to that of TE legs. Thus, a well-performing TE device requires integration of multiple layers with varying thermal expansion coefficients, thermal and electrical properties, and process compatibility. Going forward, it is vital for TE community to demonstrate high temperature and high electrical conversion efficiency (ECE) devices in order to meet the application-oriented metrics.

Recently, half-Heusler (hH) materials have been thoroughly investigated due to their excellent TE properties at high temperature, and high mechanical strength and thermal stability [46,47]. There are some promising compositions in p- and n-type hH TE materials such as ACoSb (A = Ti, Zr, Hf) [48,49] and BFeSb (B = Nb, Ta) [44,50] systems. However, there is scarcity in demonstration of reliable hH TE devices, mainly due to the high contact resistance between the metal electrode (also known as interconnect) and TE leg which is a prominent factor in determining the device ECE. Main challenges in fabricating reliable TEG device is to identify suitable metallization and brazing material in order to obtain low contact resistance [51,52,53,54]. Here we briefly list some important demonstrations in literature. Zhang *et al.* [55] demonstrated 1 kW

output power at ΔT =550°C using 400 hH TEGs where each TEG consisted of 28 unicouples. Each unicouple produced a power density of 5.26 Wcm⁻² with respect to TE leg area at ΔT of 500°C. Fu *et al*. [56] fabricated a hH device comprising of 8 unicouples which showed a maximum device power density of 2.2 Wcm⁻² and a conversion efficiency of 6.2% at ΔT =655°C. Yu *et al*. [57] built a hH module comprising of 8 unicouples which showed a power density of 2.11 Wcm⁻² with respect to the total device and a conversion efficiency of ~8.3% under a temperature difference of 655°C. Bartholomé et al. [58] fabricated a hH module comprising of 7 unicouples with a peak power density of 1.1 Wcm⁻² with respect to the total device and 3.2 Wcm⁻² with respect to the TE material at ΔT =527°C. Joshi *et al*. [53] reported hH unicouple which showed a peak power density of ~8.9 Wcm⁻² with a conversion efficiency of ~8.9% at a temperature difference of 678°C.

In order to enhance the performance of a TE device, in addition to high ΔT and $(zT)_{avg}$, device design is critical towards minimizing the thermal and electrical contact resistances at the junction of metal electrode and TE leg (semiconductor). The main source of thermal contact resistance is roughness of contact surfaces that can be minimized by finely polishing the surfaces to increase the effective contact area for thermal conduction [59]. Thermal paste can also be used to improve the thermal conduction by filling the gaps between two surfaces. The metal/semiconductor electrical contact can have Schottky (rectifying) or ohmic (non-rectifying) behavior. In TE devices, an ohmic contact behavior is crucial to provide easy conduction of electrical charges and reduce the Joule heating [31,52,53,59]. Introducing a limited diffusion barrier at the junction of Cu electrode and TE legs is a practical way to minimize atomic diffusion, control chemical reaction with TE materials and maintain conductive electrical contact [60]. However, such barriers can also generate contact resistance which can be amplified at high temperature. In general, diffusion barrier material, brazing technique and material, and difference

in coefficient of thermal expansion between TE legs and electrodes can result in high contact resistance [61], deterioration in TE properties due to the extended diffused layer and reacted TE materials at high temperature [53], and crack generation and propagation at the junction during thermal cycling [62,63].

In order to overcome the problems listed above and provide superior ECE, we demonstrate a direct bonding technique that does not require metallization of TE legs. We successfully fabricated and characterized a high temperature hH TE module comprising of nanostructured p-type ZrCoSb [64] and n-type ZrNiSn [65] legs which can withstand a hot-side temperature of ~700°C in vacuum. By reducing the specific contact resistances of both p- and n-type legs through the direct bonding technique, a 30% improvement in power density is achieved compared to the best reported data [53], with a thermal to electrical energy conversion efficiency of 9.5% at 670°C temperature gradient, which to the best of our knowledge is the highest reported efficiency for a single stage hH device made using similar p- and n-type TE materials and properties.

2. Results and Discussion

2.1. Half-Heusler Thermoelectric Module Fabrication

A thin diffusion barrier layer is commonly utilized for enabling the brazing of TE legs to metal electrodes. This is achieved by metallizing the top and bottom surface of the TE materials with a conductive metal such as gold, silver or nickel. Figure 1-a and b show common techniques for growing diffusion barrier layer. One of the methods is based upon thin film deposition techniques (Figure 1-a) such as electroplating [66], electroless plating [67,68], sputtering [69], and electron-beam evaporation [70,71]. Thin film deposition provides low contact resistance and high-temperature stability, but it is expensive process, requires long time, and there is a possibility of peeling off the metalized film. Another method is through simultaneous sintering of diffusion

barrier metal (or alloy) onto TE materials via spark plasma sintering (SPS) (Figure 1-b). Although the SPS process is convenient, it can generate extra contact resistance at the interface [72,73]. Different materials have been used as a diffusion barrier in TE modules, such as Ni in Bi₂Te₃-based modules [66,70], Mo [74]; Ti-Al [75] in skutterudite-based modules; Fe, Ni, Co and Nb-based alloys in PbTe-based modules [76,77]; and Ti in hH-based modules [53]. Even though the diffusion barrier might have a good electrical contact at room temperature, it can be a source of contact resistance at high temperature [76] that deteriorates the output power and efficiency of the TE module. Another issue that can reduce the device performance and increase the TEG fabrication cost is partial or total peeling off the metalized layer from the legs during the dicing process.

The direct bonding technique provides a sophisticated solution for the metallization of TE materials (Figure 1-c). Figure 1-d and e show the schematic and the actual fabricated unicouple TEG module made of p- and n-type hH legs, respectively. Different components of the unicouple include direct bonded copper (DBC) substrates made of copper and aluminum nitride (AlN) for top and bottom headers. AlN is a hard ceramic with high thermal conductivity and electrical insulation properties. It is used to efficiently conduct the heat from heat source to TEG as well as maintain the mechanical rigidity of the TEG. Cu electrode provides electrical conduction between TE materials. A pair of p- and n-type TE materials are connected thermally in parallel and electrically in series. Brazing material is used to provide a reliable connection between TE legs and Cu. The brazing material should have a high wettability, minimum interfacial diffusion in TE legs and high electrical and thermal conduction. Direct bonding technique enables brazing of TE legs to Cu electrode without metallizing legs. This technique reduces the module fabrication complexity, fabrication time, defects at the junction, and interfacial resistances.

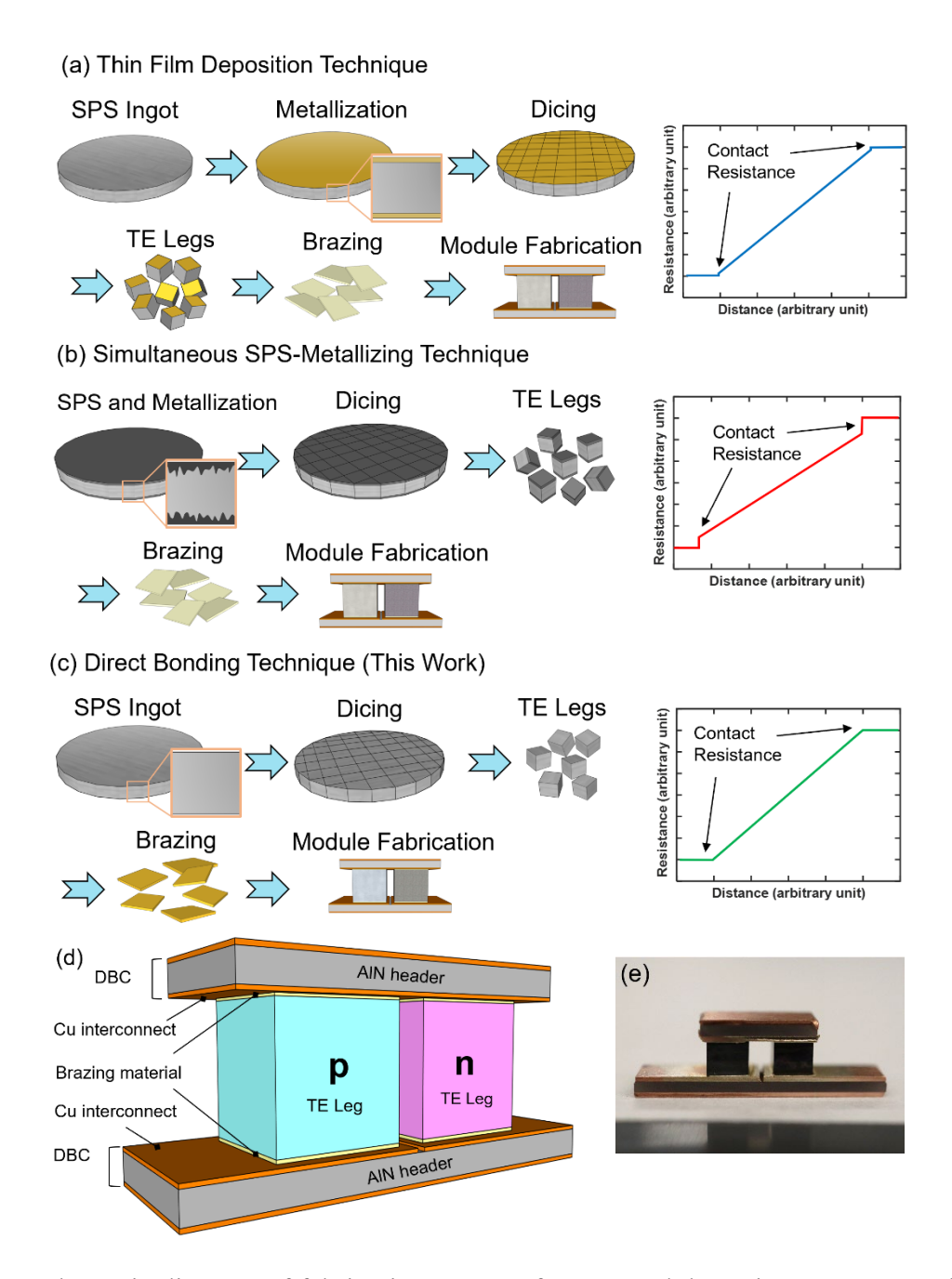


Figure 1: Schematic diagram of fabrication process for TE modules using common techniques to grow metallized (diffusion barrier) layer (a) thin film deposition technique, and (b) simultaneous sintering and metallization by SPS. Dicing the legs may peel off metallized layer in (a) and (b). (c) Fabrication process flow for direct bonding demonstrated in this study. (d) The schematic diagram and (e) actual picture of the fabricated hH TEG unicouple. More pictures on fabrication process for the module are provided in Figure S1.

2.2. Half-Heusler Thermoelectric Module Characterization

TE properties of synthesized nanostructured p-type ZrCoSb and n-type ZrNiSn are shown in Figure S2. The average zT of p- and n-type materials from 100°C to 700°C are 0.54 and 0.71, respectively. In order to verify the performance and reliability of the fabricated TE devices, two parameters are critical to measure: (*i*) the electrical contact resistance at the junction of TE leg and Cu interconnect, and (*ii*) the thermal to electrical conversion efficiency. These parameters are separately measured by home-built setups.

The relationship between the device ZT (with uppercase Z) and the material zT (with lowercase z) is given by Equation (2) [78],

$$(ZT)_d = (zT)_m \left(\frac{L}{L + 2R_c \sigma}\right) \tag{2}$$

where $(ZT)_d$ and $(zT)_m$ are device and material figure of merit, respectively, L is the length of the TE leg, R_C is the electrical contact resistance, and σ is the electrical conductivity of the TE material. $(ZT)_d$ is always less than $(zT)_m$; in an ideal case that R_C =0, $(ZT)_d$ is equal to $(zT)_m$. For a highly doped TE material with high electrical conductivity ($\sim 10^3$ Scm⁻¹), $(ZT)_d$ deteriorates with thin legs and higher R_C . Hence, according to Equation (2), in order to have a maximized device performance, R_C must be negligible. This relation validates the importance of TE device design and contact resistance. R_C is mainly controlled by the quality of contact metallization of the TE materials, soldering/brazing material, material and surface preparation of electrodes, and device fabrication process [54,79].

The effect of contact resistance is more crucial when the electrical conductivity of the TE legs is high [79]. Therefore, TE materials with high electrical conductivity requires a better contact to minimize the contact resistance. The contact resistances of both legs were analyzed using an automated scanning four-probe technique (Figure 2-a and b). The resistances of both p- and n-leg

increase linearly with distance and neither diffusion nor notable contact resistance at the interfaces are observed (Figure 2-c and d). The results show an ultra-low ohmic contact resistance between the Cu electrode and the TE legs. The specific contact resistance of p- and n-type TE legs is $<1\mu\Omega.cm^2$, which is among the lowest contact resistances in different TE materials [53,80,81]. This is also the lowest reported contact resistance in hH modules, which enables the power output and efficiency improvement [56,58]. The low contact resistance minimizes Joule heating at the interface of TE leg/Cu electrode resulting in a more efficient thermal to electrical energy conversion. The reduced contact resistance at the junction also resulted in a very low overall unicouple internal resistance of ~4 m Ω at room temperature.

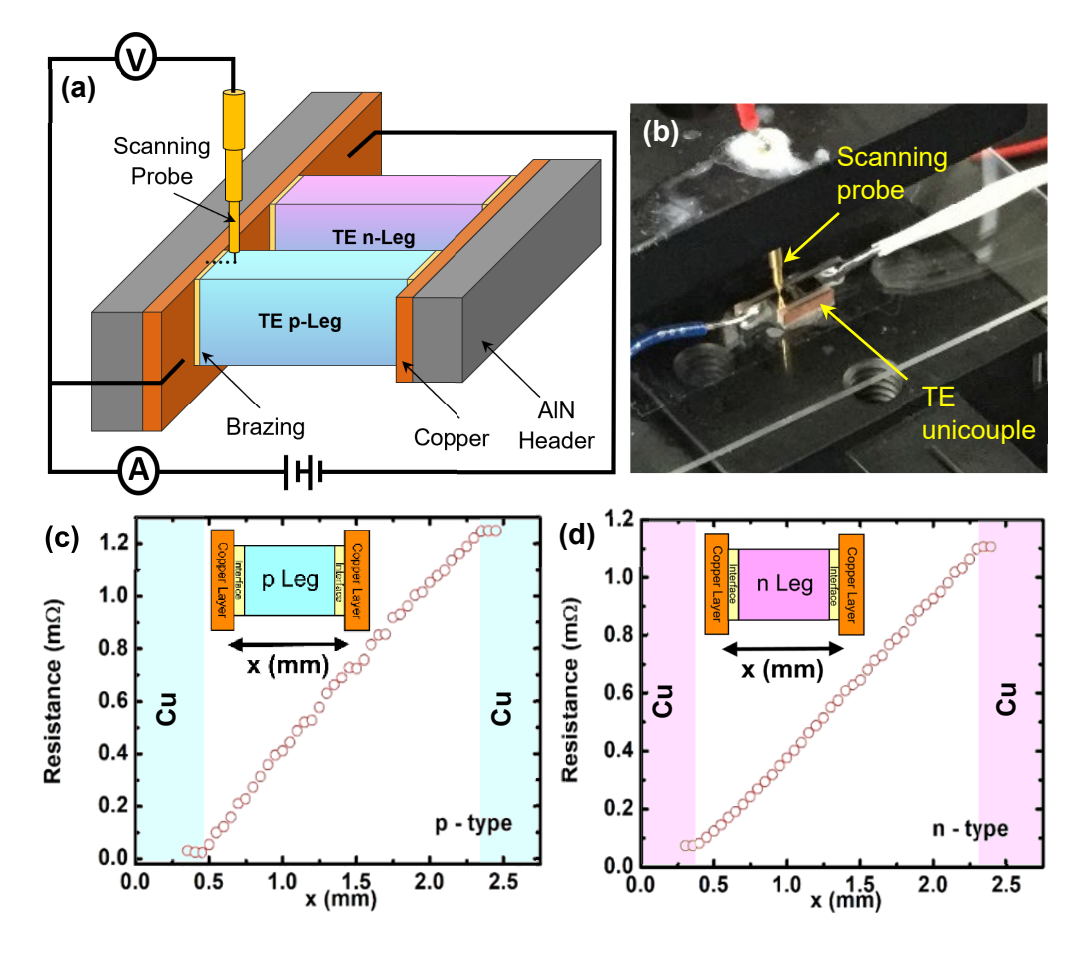


Figure 2: (a) The schematic diagram and (b) actual picture of home-made four-probe contact resistance measurement system. The contact resistance plots for (c) p-type, and (d) n-type legs.

The copper-silver (Cu-Ag) based alloy is used as brazing material to connect hH legs and copper electrode. Figure 3 shows the scanning electron microscopy (SEM) image along with elemental energy-dispersive X-ray spectroscopy (EDS) mapping for p- and n-type legs at the junction of TE leg with Cu electrode. Higher magnification SEM image and morphology of the interface are shown in Supplementary Information (Figure S3). The interface is uniform and there is no trace of any structural defect at the junction (Figure 3). Elimination of diffusion barrier resulted in limited diffusion of the brazing material into the TE legs (intermetallic layer), on the order of <20 um in p- and n-leg, which is significantly lower than the reported values for the same material system [53]. Thus, TE material properties do not deteriorate at the junction of TE leg and Cu electrode, which is a common problem in TE device fabrication due to the high temperature processing. This result matches with the contact resistance data that shows ohmic contact with negligible resistance at the junction of the TE leg/Cu electrode. Since the brazing temperature is higher than the operational temperature, the small diffusion layer helps in creating a strong intermetallic compound (mainly made of Cu, Ag and Sn) that benefits stable bonding and limits further diffusion of Cu into the legs, thereby, stabilizing the device performance.

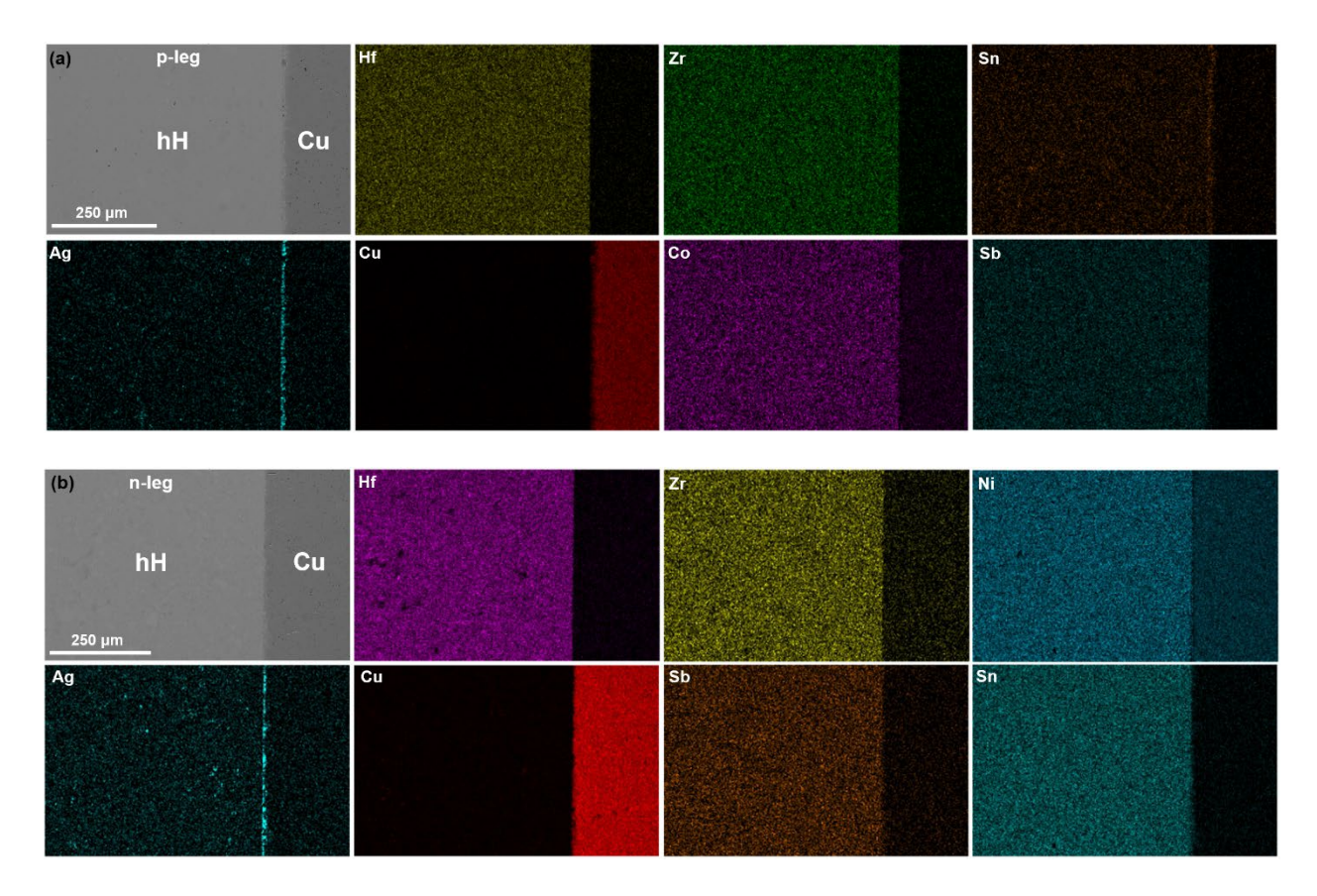


Figure 3: SEM image and EDS mapping of Cu-Ag brazing material at hH/Cu interface for (a) p-and (b) n-type hH thermoelectric legs.

The main compartments of the home-built test setup to measure the conversion efficiency of a unicouple TEG include a high temperature compatible heater assembly to provide uniform hot-side temperature, a TEG unicouple connected to power supply and voltmeter to accurately apply a load and measure voltage difference, a Q-meter to measure the heat flow at a certain distance, a water-cooled heatsink attached to the bottom of the Q-meter to maintain the cold-side temperature constant and dissipate the heat coming from the heat source (Figure S4). The temperature gradient along the Q-meter is measured with several K-type thermocouples with specific equal distances (Figure S4). The efficiency calculation equations are presented in the supplementary information. The output power and efficiency measurements were performed up to 700°C in vacuum while the cold-side temperature was maintained at ~20°C using a cooling water circulation system.

Conductive silver paste was applied at the junction of heater/top header, and thermal paste (OMEGATHERMTM) was applied at the junction of bottom header/cooler to minimize the thermal contact resistance on the hot- and cold-side, respectively. Upon increasing the hot-side temperature, output voltage, resistance, power and efficiency increased, as shown in Figure 4.

The open circuit voltage (V_{OC}) increases linearly with temperature and reaches to a maximum of 231.4 V at $\Delta T=670^{\circ}$ C (Figure 4-a). The device resistance (R) increases from 8.8 m Ω at $\Delta T=182$ °C and reaches to 11.1 m Ω at $\Delta T=670$ °C (Figure 4-b). Device voltage (V_d) shows a linear trend versus current (I) under different ΔT 's (Figure 4-c), and at I=0 A it is equal to Voc. Power density was calculated by knowing R, Voc, V_d , cross-sectional area of the thermoelectric legs, and the current (Figure 4-d). At each temperature, the maximum power is obtained from Figure 4-c or simply calculated by $P_{max} = V_{OC}^2/4R$. Figure 4-e shows the temperature dependent power density compared with the literature values. Power density reaches 11.5 Wcm⁻², which is the highest output power densities among similar TE modules with similar material zT, in the same temperature range [53,55,57,58]. The maximum conversion efficiency of ~9.5% was achieved in the fabricated unicouple which is the highest efficiency to date in this temperature range in hH single stage modules (Figure 4-f) [55,56]. Dash line is the calculated maximum theoretical conversion efficiency for comparison. The theoretical efficiency is higher than experimental values in all temperature ranges. The difference is due to several reasons including the difference between the hot-side temperature and actual leg temperature and heat losses through the TE legs due to radiation. According to this result, low contact resistance at the interfaces is a crucial factor that can significantly improve power and conversion efficiency. Table S1 compares the specification and properties of the hH unicouple investigated in this study with similar hH based TEG devices reported in the literature.

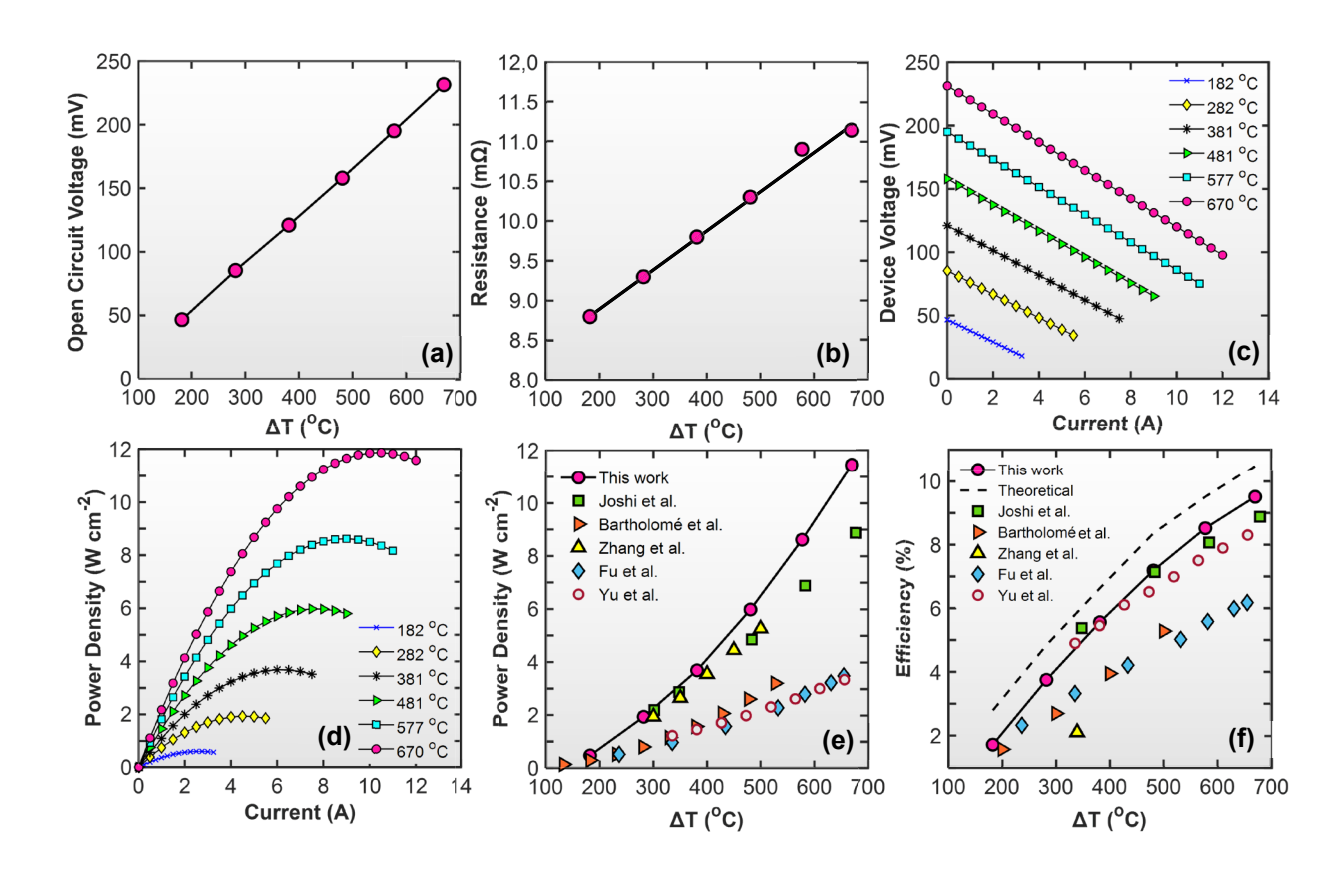


Figure 4: (a) Open circuit voltage versus ΔT , (b) resistance versus ΔT , (c) device voltage versus current (I) under different ΔT , and (d) power density of the fabricated hH unicouple versus I under different ΔT . Comparison of (e) power density with respect to the TE material, and (f) efficiency obtained in this work with hH based TEG modules reported in literature [53,55,56,57,58] as a function of ΔT .

A module comprising of 6 couples (inset of Figure 5-a), i.e., 12 n- and p-type hH legs, was fabricated and tested under similar condition in air to confirm the performance of the single couple on a larger scale. The 6 couples are electrically connected in series. Figure 5-a shows that the six-couple module produces close to 6X more power than the unicouple. This result confirms the capability of scaling this method into large-scale modules for a waste heat recovery application. One of the main obstacles to the widespread usage of TEGs is high temperature stability in a severe environment. High temperature enhances the diffused layer at contacts (the junction of leg and

headers) that degrades the overall performance of the TEGs. An oxidizing environment at high temperature also enhances the degradation rate of the TEGs by oxidizing the TE legs and deteriorating the leg/header junction. While TEGs show better performance when they are tested under vacuum in the lab environment, their practical application requires proof of operation under high temperature in-air and long-term stability. In order to validate the air stability of the modules, the unicouple was tested at a hot-side temperature of 500° C and 550° C in the air. The test setup is shown in Figure S5. No significant degradation in voltage and power was observed after more than 20 hours of operation in the air at 500° C (Figure 5), which demonstrates the high stability of the fabricated hH module in a severe environment. After 20 hours of testing at 550° C, the degradation rate is only $\sim 2.7\%$. It should be noted that the small variation between Voc and power in Figure 4 and Figure 5 is due to the difference in test conditions where usage of a large plate as a hot-side enhances radiation and convection effect that reduces ΔT across the TE leg.

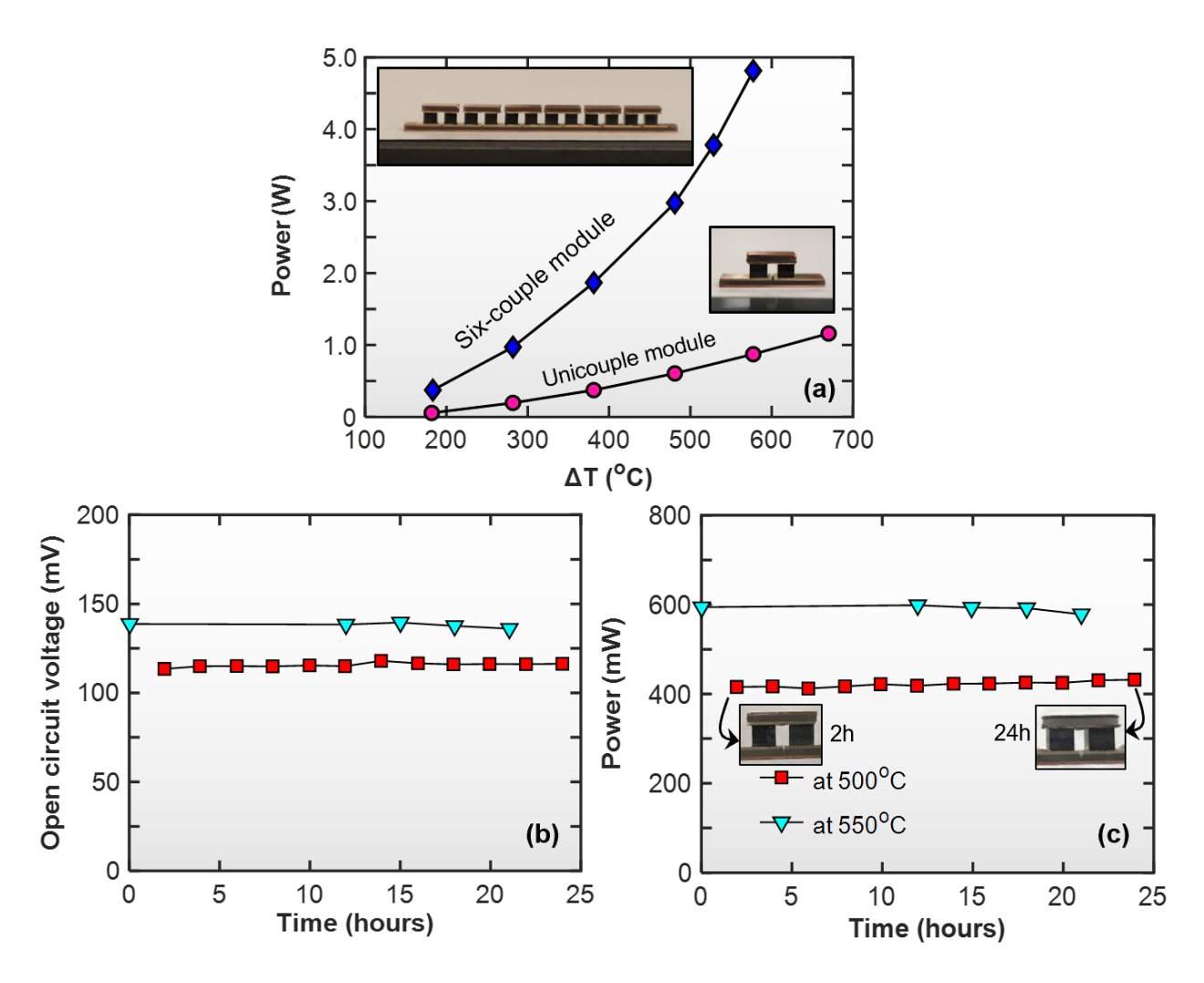


Figure 5: (a) Output power of the fabricated hH unicouple and six-couple modules versus ΔT . The inset shows the actual picture of the modules. Time dependent (b) open circuit voltage (Voc), and (c) output power of the unicouple module tested at 500 and 550°C in air. The inset shows the actual picture of the modules.

Conclusion

A thermoelectric device was fabricated from nanostructured ZrCoSb (p-type) and ZrNiSn (n-type) half-Heusler materials using a high temperature fabrication process. The joining technique successfully enabled direct bonding between TE legs and Cu electrode without leg metallization. This technique minimizes the diffusion barrier layer inside the TE leg with specific contact

resistance <1 $\mu\Omega$.cm² at the junction of leg/interconnect at room temperature. The results demonstrate the lowest contact resistance reported so far through a suitable brazing material that eliminates the time-consuming and expensive metallization process for TE legs. The peak power density of ~11.5 Wcm² and conversion efficiency of 9.5% at a temperature difference of ~670°C was achieved, which is the best performing data in rigid single stage hH alloys with similar materials to date. These results confirm the importance of the module fabrication technique to achieve low contact resistance half-Heusler TE modules. The air stability test results showed very stable performance up to 550°C, opening the opportunity to use thermoelectric generators for high temperature heat recovery application.

Experimental Section

Materials synthesis: High-purity elements of zirconium slug (Zr, 99.9%), hafnium piece (Hf, 99.9%), cobalt pieces (Co, 99.9%), nickel slug (99.995%), antimony shot (Sb, 99.999%), and tin wire (Sn, 99.95%) were used to fabricate p-type Hf_{0.5}Zr_{0.5}CoSb_{0.8}Sn_{0.2} (ZrCoSb) and n-type Hf_{0.75}Zr_{0.25}NiSn_{0.99}Sb_{0.01} (ZrNiSn) half-Heusler alloys. The alloys were synthesized by induction melting under argon atmosphere followed by high energy ball milling using SPEX mixer/mill (Model 8000D, SPEX). The synthesized p- and n-type powders were then consolidated in a cylindrical graphite die with an inner diameter of 12.7 mm (half inch) at different temperatures using spark plasma sintering (SPS) to obtain nanostructured ingots with 12.7 mm diameter and ~2 mm height. Thermoelectric properties of the synthesized materials are presented in Figure S2.

Unicouple fabrication: Nanostructured ZrCoSb (p-type) and ZrNiSn (n-type) based half-Heusler ingots were polished to a thickness of ~1.92 mm using a MULTIPREP® Allied High Tech polishing system and then diced into 2.3 mm × 2.3 mm (p-type) and 2.2 mm × 2.2 mm (n-type) legs. The module was fabricated via a direct bonding technique to bond TE legs to copper (Cu)

electrode without metallizing legs using a Cu-Ag based brazing material. The legs were brazed to

Cu electrodes by a reflow process using a vacuum reflow technique in an argon environment above

700°C.

Unicouple characterization: The internal resistance of the unicouple was measured using a four-

probe meter (MTI Corporation). The contact resistances of the fabricated unicouple was then

measured by a home-made four probe technique. The output power and conversion efficiency were

measured using a home-made efficiency testing setup [82]. The system was evacuated to a pressure

of ~10⁻⁴ mbar. Once the pressure was stabilized, the measurements were started. At a set

temperature, open circuit voltage (Voc) and device voltage (Vd) were obtained simultaneously

using a voltmeter (KEITHLEY) and a power supply (KEITHLEY 2200-20-5). The internal

resistance (R_i) and peak power of the unicouple were calculated using V_{OC} and V_d . The air stability

test was performed at different temperatures in air (Figure S5). The microstructure and elemental

line scan were studied by a field emission scanning electron microscopy (FESEM, FEI Verios),

equipped with an energy-dispersive X-ray spectroscopy (EDS, Oxford Aztec).

Supplementary Information

Supplemental figures, tables and equations can be found in supplementary information.

Notes: The authors declare no competing financial interest.

Acknowledgments

U.S., B.P. and H.Z. acknowledge the financial support from the DARPA MATRIX program

(NETS). A.N. acknowledges the financial support through NSF-CREST grant number HRD

1547771. S.P. and H.B.K. acknowledge the financial support through the Office of Naval Research

through award number N00014-20-1-2602. W.L. acknowledges the support through Army RIF

17

program. C.D. acknowledges the support through the National Science Foundation IUCRC: Center

for Energy Harvesting Materials and Systems.

References

- [5] J. Mao, H. S. Kim, J. Shuai, Z. Liu, R. He, U. Saparamadu, F. Tian, W. Liu and Z. Ren, Thermoelectric properties of materials near the band crossing line in Mg₂Sn–Mg₂Ge–Mg₂Si system, Acta Materialia, **2016**, 103, 633-642.
- [6] N. Mingo, D. Hauser, N. P. Kobayashi, M. Plissonnier and A. Shakouri, "Nanoparticle-inAlloy" Approach to Efficient Thermoelectrics: Silicides in SiGe, Nano Lett. **2009**, 9(2), 711-715.
- [7] S. Chen and Z. Ren, Recent progress of half-Heusler for moderate temperature thermoelectric applications, Materials Today, **2013**, 16, 387-395.
- [8] W. G. Zeier, A. Zevalkink, Z. M. Gibbs, G. Hautier, M. G. Kanatzidis and G. J. Snyder, Thinking Like a Chemist: Intuition in Thermoelectric Materials, Angewandte Chemie International Edition, **2016**, 55, 6826-6841.
- [9] H. J. Goldsmid, in CRC Handbook of Thermoelectrics, ed. D.M. Rowe (Boca Raton: CRC Press, 1995).
- [10] L.-D. Zhao, S.-H. Lo, Y. Zhang, H. Sun, G. Tan, C. Uher, C. Wolverton, V. P. Dravid and M. G. Kanatzidis, Ultralow Thermal Conductivity and High Thermoelectric Figure of Merit in SnSe Crystals, Nature, **2014**, 508, 373-377.
- [11] G. Tan, F. Shi, S. Hao, L.-D. Zhao, H. Chi, X. Zhang, C. Uher, C. Wolverton, V. P. Dravid, M. G. Kanatzidis, Non-equilibrium processing leads to record high thermoelectric figure of merit in PbTe–SrTe, Nat. Commun. **2016**, 7, 12167.
- [12] B. Poudel, Q. Hao, Y. Ma, Y. Lan, A. Minnich, B. Yu, X. Yan, D. Wang, A. Muto, D. Vashaee, X. Chen, J. Liu, M.S. Dresselhaus, G. Chen, Z. Ren, High-Thermoelectric Performance of Nanostructured Bismuth Antimony Telluride Bulk Alloys, Science, **2008**, 320, 634.
- [13] A. Nozariasbmarz, F. Suarez, J. H. Dycus, M. J. Cabral, J. M. LeBeau, M. C. Öztürk, D. Vashaee, Thermoelectric generators for wearable body heat harvesting: Material and device concurrent optimization, Nano Energy, **2020**, 67, 104265.
- [14] A. Nozariasbmarz, J.S. Krasinski, D. Vashaee, N-Type Bismuth Telluride Nanocomposite Materials Optimization for Thermoelectric Generators in Wearable Applications, Materials, **2019**, 12 (9), 1529.

^[1] R. He, G. Schierning and K. Nielsch, Thermoelectric Devices: A Review of Devices, Architectures, and Contact Optimization, Advanced Materials Technologies, **2018**, 3, 1700256.

^[2] G. J. Snyder and E. S. Toberer, Complex thermoelectric materials, Nature Materials, **2008**, 7, 105-114.

^[3] J. de Boor, T. Dasgupta, U. Saparamadu, E. Müller and Z. Ren, Recent progress in p-type thermoelectric magnesium silicide based solid solutions, Materials Today Energy, **2017**, 4, 105-121

^[4] U. Saparamadu, J. Mao, K. Dahal, H. Zhang, F. Tian, S. Song, W. Liu and Z. Ren, The effect of charge carrier and doping site on thermoelectric properties of Mg₂Sn_{0.75}Ge_{0.25}, Acta Materialia, **2017**, 124, 528-535.

- [15] A. Nozariasbmarz, D. Vashaee, Effect of Microwave Processing and Glass Inclusions on Thermoelectric Properties of P-Type Bismuth Antimony Telluride Alloys for Wearable Applications, Energies, **2020**, 13, 4524.
- [16] M. Wood, J. J. Kuo, K. Imasato, G. J. Snyder, Improvement of Low-Temperature zT in a Mg3Sb2–Mg3Bi2 Solid Solution via Mg-Vapor Annealing. Adv. Mater. **2019**, 31, 1902337.
- [17] J. Mao, H. Zhu, Z. Ding, Z. Liu, G. A. Gamage, G. Chen, Z. Ren, High thermoelectric cooling performance of n-type Mg3Bi2-based materials, Science, **2019**, 365, 495.
- [18] K. Imasato, C. Fu, Y. Pan, M. Wood, J. J. Kuo, C. Felser, G. J. Snyder, Metallic n-Type Mg3Sb2 Single Crystals Demonstrate the Absence of Ionized Impurity Scattering and Enhanced Thermoelectric Performance, Adv. Mater. **2020**, 32, 1908218.
- [19] X. Shi, J. Yang, S. Bai, J. Yang, H. Wang, M. Chi, J. R. Salvador, W. Zhang, L. Chen and W. Wong-Ng, Advanced Functional Materials, **2010**, 20, 755-763.
- [20] U. Saparamadu, J. de Boor, J. Mao, S. Song, F. Tian, W. Liu, Q. Zhang and Z. Ren, Comparative studies on thermoelectric properties of p-type Mg2Sn0. 75Ge0. 25 doped with lithium, sodium, and gallium, Acta Materialia, **2017**, 141, 154-162.
- [21] T. Dasgupta, C. Stiewe, J. de Boor and E. Mueller, Influence of power factor enhancement on the thermoelectric figure of merit in Mg₂Si_{0.4}Sn_{0.6} based materials, physica status solidi (a), **2014**, 211, 1250-1254.
- [22] S. Kim, B. Wiendlocha, H. Jin, J. Tobola and J. P. Heremans, Electronic structure and thermoelectric properties of p-type Ag-doped Mg₂Sn and Mg₂Sn_{1-x}Si_x (x = 0.05, 0.1), Journal of Applied Physics, **2014**, 116, 153706.
- [23] J.-L. Lan, Y.-C. Liu, B. Zhan, Y.-H. Lin, B. Zhang, X. Yuan, W. Zhang, W. Xu and C. W. Nan, Enhanced Thermoelectric Properties of Pb-doped BiCuSeO Ceramics, Advanced Materials, **2013**, 25, 5086-5090.
- [24] L.-D. Zhao, J. He, D. Berardan, Y. Lin, J.-F. Li, C.-W. Nan and N. Dragoe, BiCuSeO oxyselenides: new promising thermoelectric materials, Energy & Environmental Science, **2014**, 7, 2900-2924.
- [25] B. Ren, M. Liu, X. G. Li, X. Y. Qin, D. Li, T. Zou, G. L. Sun, y. Li, H. X. Xin and J. Zhang, Enhancement of thermoelectric performance of b-Zn4Sb3 through resonant distortion of electronic density of states doped with Gd, Journal of Materials Chemistry A, **2015**, 3, 11768-11772.
- [26] T. H. Zou, X. Y. Qin, D. Li, B. J. Ren, G. L. Sun, Y. C. Dou, Y. Y. Li, L. Li, J. Zhang and H. X. Xin, Enhanced thermoelectric performance via carrier energy filtering effect in β-Zn4Sb3 alloy bulk embedded with (Bi₂Te₃)_{0.2}(Sb₂Te₃)_{0.8}, Journal of Applied Physics, **2014**, 115, 053710.
- [27] H. Liu, X. Yuan, P. Lu, X. Shi, F. Xu, Y. He, Y. Tang, S. Bai, W. Zhang, L. Chen, Y. Lin, L. Shi, H. Lin, X. Gao, X. Zhang, H. Chi and C. Uher, Ultrahigh Thermoelectric Performance by Electron and Phonon Critical Scattering in Cu₂Se_{1-x}I_x, Advanced Materials, **2013**, 25, 6607-6612.
- [28] B. Yu, W. Liu, S. Chen, H. Wang, H. Wang, G. Chen and Z. Ren, Thermoelectric properties of copper selenide with ordered selenium layer and disordered copper layer, Nano Energy, **2012**, 1, 472-478.
- [29] W.-D. Liu, D.-Z. Wang, Q. F. Liu, W. Zhou, Z. Shao, Z.-G. Chen, High-Performance GeTe-Based Thermoelectrics: from Materials to Devices, Adv. Energy Mater. **2020**, 10, 2000367.
- [30] J. Li, X. Zhang, Z. Chen, S. Lin, W. Li, J. Shen, I. T. Witting, A. Faghaninia, Y. Chen, A. Jain, L. Chen, G. J. Snyder, Y. Pei, Low-Symmetry Rhombohedral GeTe Thermoelectrics, Joule, **2018**, 2, 976.
- [31] A. Rao, G. Bosak, B. Joshi, J. Keane, L. Nally, A. Peng, S. Perera, A. Waring and B. Poudel, A TiAlCu Metallization for 'n' Type CoSb_x Skutterudites with Improved Performance for High-

- Temperature Energy Harvesting Applications, Journal of Electronic Materials, **2017**, 46, 2419-2431.
- [32] G. Rogl, A. Grytsiv, K. Yubuta, S. Puchegger, E. Bauer, C. Raju, R. C. Mallik and P. Rogl, In-doped multifilled n-type skutterudites with ZT = 1.8, Acta Materialia, **2015**, 95, 201-211.
- [33] W. Li, J. Wang, Y. Xie, J. L. Gray, J. J. Heremans, H. B. Kang, B. Poudel, S. T. Huxtable and S. Priya, Enhanced Thermoelectric Performance of Yb-Single-Filled Skutterudite by Ultralow Thermal Conductivity, Chem Mater, **2019**, 31, 862-872.
- [34] W. Li, D. Stokes, B. Poudel, U. Saparamadu, A. Nozariasbmarz, H. B. Kang, S. Priya, High-Efficiency Skutterudite Modules at a Low Temperature Gradient, Energies, **2019**, 12 (22), 4292.
- [35] G. Nie, W. Li, J. Guo, A. Yamamoto, K. Kimura, X. Zhang, E. B. Isaacs, V. Dravid, C. Wolverton, M. G. Kanatzidis, S. Priya, High performance thermoelectric module through isotype bulk heterojunction engineering of skutterudite materials. Nano Energy, **2019**, 66, 104193.
- [36] G. Joshi, H. Lee, Y. Lan, X. Wang, G. Zhu, D. Wang, R. W. Gould, D. C. Cuff, M. Y. Tang and M. S. Dresselhaus, G. Chen, Z. Ren, Enhanced Thermoelectric Figure-of-Merit in Nanostructured p-type Silicon Germanium Bulk Alloys, Nano letters, **2008**, 8, 4670-4674.
- [37] A. Nozariasbmarz, P. Roy, Z. Zamanipour, J.H. Dycus, M.J. Cabral, J.M. LeBeau, J.S. Krasinski, D. Vashaee, Comparison of thermoelectric properties of nanostructured Mg2Si, FeSi2, SiGe, and nanocomposites of SiGe–Mg2Si, SiGe–FeSi2, Apl. Mater. **2016**, 4, 104814.
- [38] A. Nozariasbmarz, Z. Zamanipour, P. Norouzzadeh, J. S. Krasinski and D. Vashaee, Enhanced thermoelectric performance in a metal/semiconductor nanocomposite of iron silicide/silicon germanium, RSC Advances, **2016**, 6 (55), 49643-49650.
- [39] A. Nozariasbmarz, A. Agarwal, Z. A. Coutant, M. J. Hall, J. Liu, R. Liu, A. Malhotra, P. Norouzzadeh, V. P. Ramesh, Y. Sargolzaeiaval, F. Suarez, M. C. Öztürk, D. Vashaee, Thermoelectric Silicides: A Review, Japanese Journal of Applied Physics, **2017**, 56, 05DA04.
- [40] S. R. Brown, S. M. Kauzlarich, F. Gascoin and G. J. Snyder, Chemistry Of Materials, 2006, 18, 1873-1877.
- [41] H. Xie, H. Wang, C. Fu, Y. Liu, G. J. Snyder, X. Zhao and T. Zhu, The intrinsic disorder related alloy scattering in ZrNiSn half-Heusler thermoelectric materials, Sci. Rep. **2014**, 4, 6888.
- [42] W. Ren, H. Zhu, Q. Zhu, U. Saparamadu, R. He, Z. Liu, J. Mao, C. Wang, K. Nielsch, Z. Wang and Z. Ren, Ultrahigh Power Factor in Thermoelectric System Nb_{0.95}M_{0.05}FeSb (M = Hf, Zr, and Ti), Advanced Science **2018**, 5, 1800278.
- [43] G. Joshi, R. He, M. Engber, G. Samsonidze, T. Pantha, E. Dahal, K. Dahal, J. Yang, Y. Lan, B. Kozinsky and Z. Ren, NbFeSb-based p-type half-Heuslers for power generation applications, Energy & Environmental Science **2014**, 7, 4070-4076.
- [44] H. Zhu, J. Mao, Y. Li, J. Sun, Y. Wang, Q. Zhu, G. Li, Q. Song, J. Zhou, Y. Fu, R. He, T. Tong, Z. Liu, W. Ren, L. You, Z. Wang, J. Luo, A. Sotnikov, J. Bao, K. Nielsch, G. Chen, D. J. Singh and Z. Ren, Discovery of TaFeSb-based half-Heuslers with high thermoelectric performance, Nat. Commun. 2019, 10, 270.
- [45] H. B. Kang, B. Poudel, W. Li, H. Lee, U. Saparamadu, A. Nozariasbmarz, M. G. Kang, A. Gupta, J. J. Heremans and S. Priya, Decoupled phononic-electronic transport in multi-phase n-type half-Heusler nanocomposites enabling efficient high temperature power generation, Mater. Today, **2020**, 36, 63-72.
- [46] J. Yu, K. Xia, X. Zhao and T. Zhu, High performance p-type half-Heusler thermoelectric materials, Journal of Physics D: Applied Physics, **2018**, 51, 113001.

- [47] R. He, D. Kraemer, J. Mao, L. Zeng, Q. Jie, Y. Lan, C. Li, J. Shuai, H. S. Kim and Y. Liu, D. Broido, C.-W. Chu, G. Chen, Z. Ren, High power factor and power density in NbFeSb, Proceedings of the National Academy of Sciences, **2016**, 113, 13576-13581.
- [48] N. Chauhan, A. Bhardwaj, T. Senguttuvan, R. Pant, R. Mallik and D. Misra, Journal of Materials Chemistry C, **2016**, 4, 5766-5778.
- [49] Y. Xia, V. Ponnambalam, S. Bhattacharya, A. L. Pope, S. J. Poon and T. M. Tritt, Journal Of Physics-Condensed Matter, **2001**, 13, 77-89.
- [50] J. Yu, C. Fu, Y. Liu, K. Xia, U. Aydemir, T. C. Chasapis, G. J. Snyder, X. Zhao and T. Zhu, Advanced Energy Materials **2018**, 8, 1701313.
- [51] W. Liu, Q. Jie, H. S. Kim and Z. Ren, Current progress and future challenges in thermoelectric power generation: From materials to devices, Acta Materialia, **2015**, 87, 357-376.
- [52] D. Ben-Ayoun, Y. Sadia and Y. Gelbstein, Compatibility between Co-Metallized PbTe Thermoelectric Legs and an Ag-Cu-In Brazing Alloy, Materials, **2018**, 11, 99.
- [53] G. Joshi and B. Poudel, Efficient and Robust Thermoelectric Power Generation Device Using Hot-Pressed Metal Contacts on Nanostructured Half-Heusler Alloys, Journal of Electronic Materials, **2016**, 45, 6047-6051.
- [54] W. Li, B. Poudel, A. Nozariasbmarz, R. Sriramdas, H. Zhu, H. B. Kang, S. Priya, Bismuth Telluride/Half-Heusler Segmented Thermoelectric Unicouple Modules Provide 12% Conversion Efficiency, Advanced Energy Materials, **2020**, 2001924.
- [55] Y. Zhang, M. Cleary, X. Wang, N. Kempf, L. Schoensee, J. Yang, G. Joshi and L. Meda, High-temperature and high-power-density nanostructured thermoelectric generator for automotive waste heat recovery, Energy Conversion and Management, **2015**, 105, 946-950.
- [56] C. Fu, S. Bai, Y. Liu, Y. Tang, L. Chen, X. Zhao and T. Zhu, Realizing high figure of merit in heavy-band p-type half-Heusler thermoelectric materials, Nature communications, **2015**, 6, 8144.
- [57] J. Yu, Y. Xing, C. Hu, Z. Huang, Q. Qiu, C. Wang, K. Xia, Z. Wang, S. Bai, X. Zhao, L. Chen and T. Zhu, Half-Heusler Thermoelectric Module with High Conversion Efficiency and High Power Density, Adv. Energy Mater. **2020**, 2000888.
- [58] K. Bartholomé, B. Balke, D. Zuckermann, M. Köhne, M. Müller, K. Tarantik and J. König, Thermoelectric Modules Based on Half-Heusler Materials Produced in Large Quantities, Journal of Electronic Materials, **2014**, 43, 1775-1781.
- [59] R. He, G. Schierning, K. Nielsch, Thermoelectric Devices: A Review of Devices, Architectures, and Contact Optimization, Adv. Mater. Technol. **2018**, 3, 1700256.
- [60] G. Tan, M. Ohta, M. G. Kanatzidis, Thermoelectric power generation: from new materials to devices, Phil. Trans. R. Soc. A, **2019**, 377, 20180450.
- [61] P. H. Ngan, N. Van Nong, L. T. Hung, B. Balke, L. Han, E. M. J. Hedegaard, S. Linderoth, N. Pryds, On the Challenges of Reducing Contact Resistances in Thermoelectric Generators Based on Half-Heusler Alloys. J. Electron. Mater. **2016**, 45, 594-601.
- [62] S. H. Park, Y. Jin, K. Ahn et al. Ag/Ni Metallization Bilayer: A Functional Layer for Highly Efficient Polycrystalline SnSe Thermoelectric Modules. Journal of Electronic Materials **2017**, 46, 848–855.
- [63] Y. Kim, G. Yoon, B. J. Cho, S. H. Park, Multi-Layer Metallization Structure Development for Highly Efficient Polycrystalline SnSe Thermoelectric Devices, Appl. Sci. **2017**, 7(11), 1116.
- [64] X. Yan, G. Joshi, W. Liu, Y. Lan, H. Wang, S. Lee, J. Simonson, S. Poon, T. Tritt, G. Chen, and Z. F. Ren, Enhanced Thermoelectric Figure of Merit of p-Type Half-Heuslers, Nano letters, **2011**, 11, 556-560.

- [65] G. Joshi, X. Yan, H. Wang, W. Liu, G. Chen and Z. Ren, Enhancement in Thermoelectric Figure-Of-Merit of an N-Type Half-Heusler Compound by the Nanocomposite Approach, Advanced Energy Materials, **2011**, 1, 643-647.
- [66] L. Chen, D. Mei, Y. Wang, L. Yang, Ni barrier in Bi2Te3-based thermoelectric modules for reduced contact resistance and enhanced power generation properties, J. Alloys Compd. **2019**, 796, 314-320.
- [67] P.Y. Chien, C.H. Yeh, H. H. Hsu et al., Polarity Effect in a Sn3Ag0.5Cu/Bismuth Telluride Thermoelectric System. Journal of Elec Materials, **2014**, 43, 284-289.
- [68] W. Lin, Y. Li, A. T. Wu, Study of Diffusion Barrier for Solder/n-Type Bi2Te3 and Bonding Strength for p- and n-Type Thermoelectric Modules. Journal of Elec Materials, **2018**, 47, 148-154.
- [69] O. D. Iyore, T. H. Lee, R. P. Gupta, J. B. White, H. N. Alshareef, M. J. Kim, B. Gnade, Interface characterization of nickel contacts to bulk bismuth tellurium selenide. Surf. Interface Anal. **2009**, 41, 440-444.
- [70] R.P. Gupta, K. Xiong, J.B. White, Kyeongjae. Cho, H.N. Alshareef, and B.E. Gnade, Low Resistance Ohmic Contacts to Bi2Te3 Using Ni and Co Metallization, J. Electrochem. Soc. **2010**, 157, H666.
- [71] W. P. Lin, D. E. Wesolowski, C. C. Lee, Barrier/bonding layers on bismuth telluride (Bi2Te3) for high temperature thermoelectric modules. J Mater Sci: Mater Electron, **2011**, 22, 1313-1320.
- [72] A. Singh, S. Bhattacharya, C. Thinaharan, D. K. Aswal, S. K. Gupta, J. V. Yakhmi, K. Bhanumurthy, Development of low resistance electrical contacts for thermoelectric devices based on n-type PbTe and p-type TAGS-85 ((AgSbTe2)0.15(GeTe) 0.85), J. Phys. D. Appl. Phys. **2009**, 42, 15502:1-6.
- [73] X. R. Ferreres, S. A. Yamini, Rapid fabrication of diffusion barrier between metal electrode and thermoelectric materials using current-controlled spark plasma sintering technique, Journal of Materials Research and Technology, **2019**, 8, 8-13.
- [74] J. R. Salvador et al., Conversion efficiency of skutterudite-based thermoelectric modules. Phys. Chem. Phys. **2014**, 16, 12510-12520.
- [75] Q. Zhang et al., Realizing a thermoelectric conversion efficiency of 12% in bismuth telluride/skutterudite segmented modules through full-parameter optimization and energyloss minimized integration, Energy Environ. Sci. **2017**, 10, 956-963.
- [76] P. Jood, M. Ohta, A. Yamamoto, M. G. Kanatzidis, Excessively doped PbTe with Ge-induced nanostructures enables high-efficiency thermoelectric modules, Joule, **2018**, 2, 1339-1355.
- [77] G. Tan, M. Ohta, M. G. Kanatzidis, Thermoelectric power generation: from new materials to devices, Phil. Trans. R. Soc. A, **2019**, 377, 20180450.
- [78] L. I. Anatychuk and O. J. Luste, Physical principles of microminiaturization in thermoelectricity, in 15th International Conference on Thermoelectrics, IEEE, **1996**, 279-287.
- [79] A. Nozariasbmarz, R. A. Kishore, B. Poudel, U. Saparamadu, W. Li, R. Cruz, and S. Priya, High Power Density Body Heat Energy Harvesting, ACS Appl. Mater. Inter. **2019**, 11, 43, 40107-40113.
- [80] J. de Boor, C. Gloanec, H. Kolb, R. Sottong, P. Ziolkowski and E. Müller, Fabrication and characterization of nickel contacts for magnesium silicide based thermoelectric generators, Journal of Alloys and Compounds, **2015**, 632, 348-353.
- [81] R. P. Gupta, R. McCarty and J. Sharp, Practical Contact Resistance Measurement Method for Bulk Bi2Te3-Based Thermoelectric Devices, Journal of Electronic Materials, **2014**, 43, 1608-1612.

[82] R. Ashwin, B. Pawan, B. Gregg, J. Binay, K. Jennifer, N. Luke, P. Adam, P. Susanthri, W. Alfred, J. Giri and B. Poudel, A quick and efficient measurement technique for performance evaluation of thermoelectric materials, Measurement Science and Technology, **2016**, 27, 105008.